Weak and slow, strong and fast: How shear zones evolve in a dry continental crust (Musgrave Ranges, Central Australia)

F. Hawemann[1], N. S. Mancktelow[1], G. Pennacchioni[2], S. Wex[1], A. Camacho[3],

[1]Department of Earth Sciences, ETH Zurich, Sonneggstrasse 5, 8092 Zürich, Switzerland.

[2]Department of Geosciences, University of Padova, Via Gradenigo 6, 35131 Padova, Italy.

[3] Department of Geological Sciences, University of Manitoba, 125 Dysart Rd, Winnipeg, Manitoba, R3T 2N2, Canada.

Corresponding author: Friedrich Hawemann (friedrich.hawemann@erdw.ethz.ch)

This is a non-peer reviewed preprint, submitted to

Journal of Geophysical Research - Solid Earth

Key Points:

- Ductile shearing localizes on precursor pseudotachylytes and fractures.
- Stress fluctuations range from 10 MPa to at least <1 GPa
- Earthquakes in the lower crust can be locally triggered by stress concentrations without the transfer of stresses from the upper crust.

Keywords

Pseudotachylyte, lower crust, localization of deformation, stress, earthquake

Abstract

The Davenport Shear Zone in Central Australia is a strike-slip fault zone developed during the Petermann Orogeny (~ 550 Ma) in an intracontinental lower crustal setting, with conditions of shearing estimated at upper amphibolite to eclogite facies (~ 650 °C, 1.2 GPa). This five kilometer thick mylonite zone encloses several large low-strain domains, allowing a thorough study of the initiation of shear zones and their progressive development. Quartzo-feldspathic gneisses and granitoids contain rheologically different layers, such as quartz-rich pegmatite dykes, mafic bands and dykes, which should preferentially localize viscous deformation if favourably orientated. This is not observed, except for long, continuous and fine grained dolerite dykes. Instead, many shear zones, typically only a few millimeters to centimeters in width but extending for tens of meters, commonly exploited pseudotachylytes and are sometimes parallel to a network of little overprinted brittle fractures. The recrystallized mineral assemblage in the sheared pseudotachylyte is similar to that in the host gneiss, without associated fluid-rock interaction. Lack of localization in quartz-rich, coarser grained (typically >50 microns) rocks compared to mafic dykes, precursor factures and pseudotachylytes implies that localization in the dry lower crust preferentially occurs along elongate planar layers with a relatively fine grain size. Transient high stress events repeatedly initiated fractures, providing finer grained, weaker, planar precursors that localized subsequent ductile shear zones. This intimate interplay between brittle and ductile deformation suggests a local source for lower crustal earthquakes, rather than downward migration of earthquakes from the shallower, usually more seismogenic part of the crust.

1 Introduction

In simplified one-dimensional, constant strain-rate models of lithospheric strength (e.g. Goetze and Evans, 1979), depth variation in flow stress due to crystal-plastic flow is, for a specific rock composition, assumed to be controlled by temperature. Typically, laboratory determined flow laws for wet quartz are used to model the strength of uniform crust (e.g. Kirby, 1983) or quartz and plagioclase/diabase/granulite for a two layer crust (e.g. Jackson, 2002a; Ranalli & Murphy, 1987; Burov & Watts, 2006). The simplest model of a quartz-only crust predicts the transition from dominantly brittle failure to dominantly ductile flow at about 300 °C, equivalent to a depth of 10-15 km, which is taken to be the base of the seismogenic zone (e.g. Nazareth and Hauksson, 2004; Sibson, 1982). Below this zone, rocks

are expected to flow homogenously with decreasing strength at increasing temperature. While most laboratory data is derived from wet quartz, there are petrological arguments that large parts of the lower crust may be effectively dry (Yardley and Valley, 1994, 1997). Similarly, field observations demonstrate that strain can be strongly partitioned and localized in such dry lower crust (Austrheim, 1987; Menegon et al., 2014, White, 2004).

Shear zone nucleation and strain localization in the lower crust have a major impact on the architecture of mountain belts and the study of these processes yields insights into the rheology of the Earth's crust. Shear zone nucleation requires an initial perturbation in rock viscosity, with strain localization being the result of both this initial difference and the effect of subsequent weakening mechanism(s) during the ensuing deformation. This implies that shear zones should nucleate along pre-existing lithological and rheological heterogeneities, with shearing preferentially concentrated within weaker tabular features such as mafic dykes, quartz veins and mica rich layers, or at the boundaries of stronger layers, e.g. aplite dykes, feldspar rich pegmatites (Christiansen & Pollard, 1997; Mancktelow & Pennacchioni, 2005, 2013; Pennacchioni, 2005; Pennacchioni & Mancktelow, 2007; Pennacchioni & Zucchi, 2013) During ongoing deformation, strain localization may be enhanced by increased permeability within the shear zone (Getsinger et al., 2013; Stewart et al., 2000), promoting influx of water and thereby hydrolytic (Griggs, 1967; Kronenberg et al., 1990) and reaction weakening processes, such as the breakdown of feldspar to white mica (Goncalves et al., 2012; Gueydan et al., 2003). Development of a crystallographic preferred orientation and grain size reduction can result either in strain weakening or hardening, depending on the change of deformation mechanism and the critical grain size reached (Hirth & Tullis, 1992; Kilian et al., 2011; de Raadt et al., 2014). Shear heating could also play an important role in shear localization, as has been demonstrated in numerical models (Duretz et al., 2015; Thielmann et al., 2015), but is generally predicted to be more important at larger length scales and high differential stress (Braeck and Podladchikov, 2007; Kaus and Podladchikov, 2006). The role of precursor fractures in shear zone nucleation and strain localization has been widely recognized in mid-crustal environments (Guermani and Pennacchioni, 1998; Mancktelow and Pennacchioni, 2005; Pennacchioni et al., 2006; Pennacchioni and Mancktelow, 2007; Pennacchioni and Zucchi, 2013; Schrank et al., 2008; Sibson, 1980) and to a more limited extent in the lower crust (Austrheim et al., 1996; Menegon et al., 2017; Steltenpohl et al., 2006). An interplay between "transient discontinuities", marked by pseudotachylyte formation, and ongoing ductile shear interpreted to occur under middle to lower crustal conditions, has also been described in a limited number of previous studies (Hobbs et al., 1986; Menegon et al., 2017; Sibson, 1980; White 1996, 2004, 2012).

Here we present field evidence from a well-exposed and extensive lower crustal section in the Musgrave Ranges of Central Australia to establish that (1) deformation conditions are effectively dry, without significant water-rich fluid infiltration and weakening due to hydration; (2) deformation is very heterogeneous and localized; and (3) transient high stress and related fractures provided the necessary planar precursors on which narrow ductile shear zones subsequently localized. We present a model for a heterogeneously sheared dry lower crust involving cycles of brittle and ductile deformation leading to the repeated nucleation of shear zones and strain localization.

2 Geological Overview

The Musgrave Block is located in Central Australia (Fig. 1), straddles the border between the Northern Territory and South Australia (at latitude 26°S) and extends into Western Australia (Fig. 2a). The working area is located in the central Musgrave Ranges, spanning about 50 km from east to west (Fig. 2b). A more complete overview of the metamorphic and intrusive history of the Musgrave Block can be found in Camacho (1997), Edgoose et al. (2004), Wade et al. (2008) and Howard et al. (2015). The oldest rocks in the Musgrave Block are felsic gneisses (acidic volcanic protolith), which are dated by SHRIMP U-Pb Zircon to be about 1550 Ma (Camacho & Fanning, 1995; Gray, 1978). Emplacement of these dominantly felsic rocks is succeeded in the Musgrave Block by the 1120-1220 Ma Musgravian Orogeny, which reached amphibolite facies conditions in the north (Mulga Park Subdomain) and granulite facies metamorphism in the south (Fregon Subdomain, Camacho and Fanning, 1995; Collerson et al., 1972; Major, 1973). Metamorphism is accompanied by voluminous syn- to post-tectonic granitoid intrusion assigned to the Pitjantjatjara Supersuite (Smithies et al., 2011). The magmatic history continued during the 1090-1040 Ma Giles Event (Edgoose et al., 2004; Evins et al., 2010), which can be subdivided into at least eight phases, comprising intrusions of granitoid, gabbro, norite and doleritic dykes and sills (Evins et al., 2010). In the central Musgrave Ranges, the most significant of these intrusions form the Mount Woodroffe Norite Group (Camacho 1997; Major 1973) and the widespread Alcurra (or Kulgera) dolerite dyke swarm, dated at ~1070 Ma (Camacho et al., 1991; Schmidt et al., 2006; Zhao and McCulloch, 1993). Another dolerite dyke swarm, the ~ 800 Ma Amata suite (Wingate et al., 1998; Zhao & McCulloch, 1993), also occurs in the area but the two suites are not readily distinguishable in the field, although they are chemically and isotopically distinct (Camacho 1997; Zhao et al., 1994; Zhao & McCulloch, 1993).

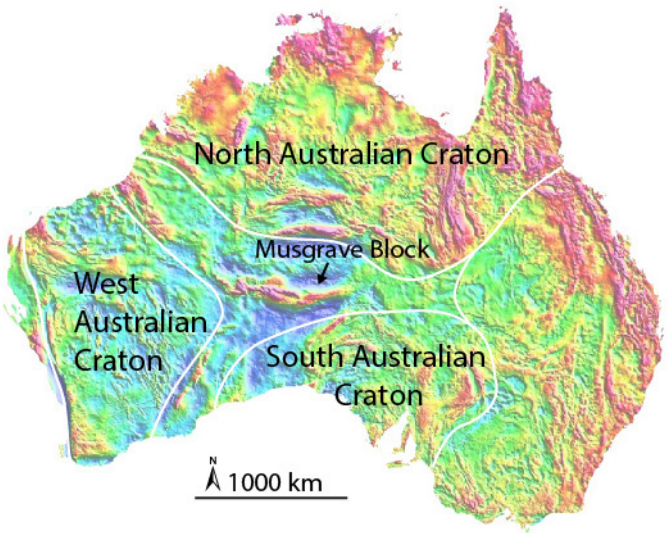

Figure 1: The position of the Musgrave Block in between the Australian Cratons. Isostatic residual gravity anomaly map by Nakamura et al. (2011), craton boundaries and Tasman Line from Evins et al. (2010).

During the intracontinental 560-520 Ma Petermann Orogeny, the Fregon Subdomain was juxtaposed against the Mulga Park Subdomain across the south-dipping Woodroffe Thrust (Camacho et al., 1995; Collerson et al., 1972; Maboko et al., 1992). The Fregon Subdomain in the hanging wall is heterogeneously overprinted by generally strike-slip shear zones, with strain strongly partitioned and localized on all scales. This shearing occurred under sub-

eclogite facies conditions of about 650 °C and 1.2 GPa (Camacho et al., 1997; Hawemann et al., 2018). Pseudotachylytes are abundant and multiple generations can pre-, syn- or post-kinematic with regard to the ductile shearing (Hawemann et al., 2018). Several larger structures have previously been named. The North Davenport Shear Zone (NDSZ) is defined as an E-W trending shear zone of limited width (Fig. 2b, Camacho et al., 1997). Further to the south, the Davenport Shear Zone (DSZ) comprises a mylonite zone of approximately five kilometer thickness (Collerson et al., 1972). The DSZ is bounded to the south by the almost parallel Mann Fault (MF), on which dextral movement most likely created the pull-apart Levenger Basin (LB, Fig. 2b; e.g. Camacho & McDougall, 2000; Major & Conor, 1993). Towards the east, deformation in the Fregon Subdomain is mainly limited to the Ferdinand Shear Zone (Fig. 2b; Camacho & Fanning, 1995).

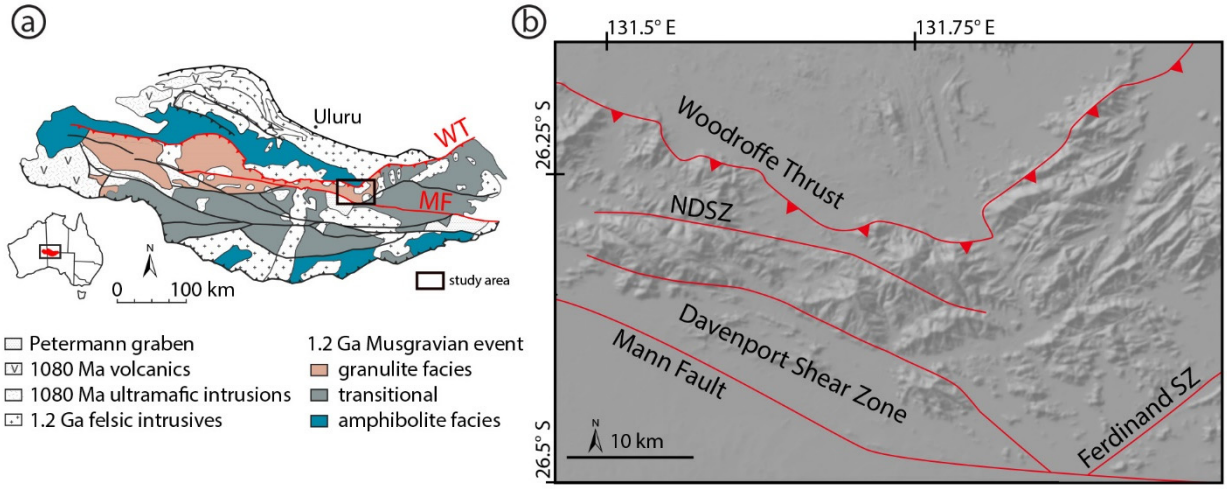

Figure 2: a) Geological map of the Musgrave Block, modified from Raimondo et al. (2010). b) Shaded relief map of the study area with large scale shear zones.

The mylonitic foliation of the DSZ is WNW-ESE trending with a slight bend into a more SE trend towards the east, which is easily discernible from airborne imagery (Fig. 3). The earlier granulite-facies foliation, locally with evident regional-scale isoclinal and intrafolial folds, is generally steeply dipping and trends almost N-S. The DSZ foliation is locally flat lying, and generally steepens towards the north, with a consistently sub-horizontal stretching lineation towards ESE or WNW (area III in Fig. 3). Shear zones with opposite sense of shear can be observed and their orientation can be used to infer the corresponding direction of bulk shortening. The angle between sinistral and dextral shear zones can be very low, but consistently indicates NNE-SSW-directed shortening (area I in Fig. 3). In comparison, areas I and III show the same direction of shortening but a slightly different orientation of the main foliation, consistent with the observation that the sense of shear on the main foliation is changing from dominantly sinistral in the W to dominantly dextral in the E. In contrast, one of the Musgravian granitic intrusions forms a low strain domain (area II in Fig. 3), and several narrow but long shear zones indicate shortening in the direction NNW-SSE. Area IV indicates a shortening direction towards NE-SW and a sinistral sense of shear. The NDSZ was studied only in a few outcrops because of difficult accessibility. It has a moderately dipping foliation towards the south with a large scatter in the lineation orientation, varying from a shallow E-W plunge to nearly down dip with dominantly dextral plus south-side-up oblique slip kinematics (area VI in Fig. 3).

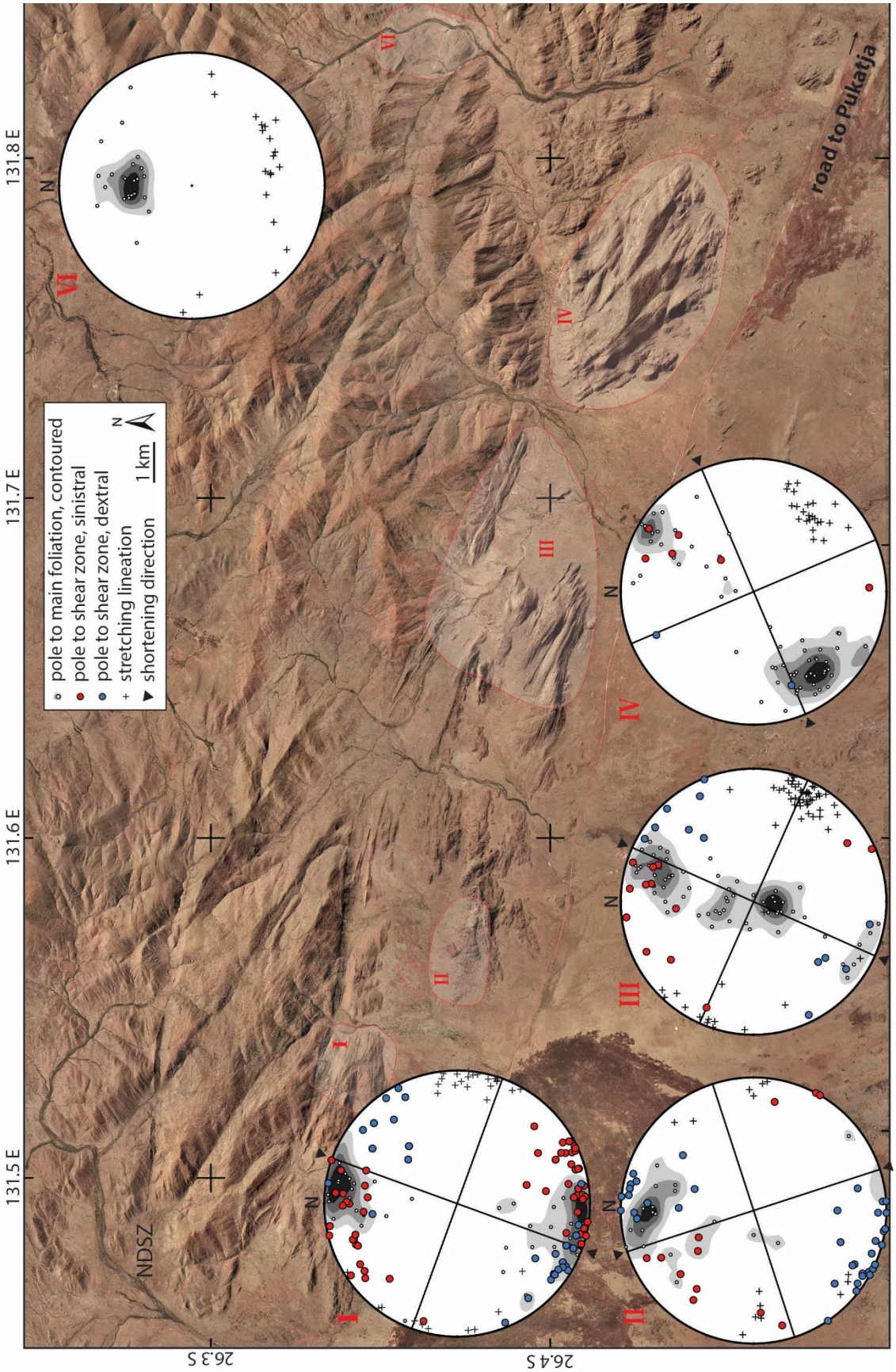

Figure 3: Airborne imagery of the Davenport Shear Zone from Department of Primary Industries and Regions, South Australia (PIRSA), 2012. Stereoplots (equal area, lower hemisphere projection) give the orientation data for the

foliation, lineation and localized shear zones associated with the Petermann Orogeny, for selected areas, with poles to sinistral shear zones indicated in red and dextral shear zones in blue.

3 Methods

Outcrops were documented using photographs and, where appropriate, by photogrammetry using the software Agisoft PhotoScan. This allows the analysis of georeferenced outcrops and preservation of shear zone geometry up to about 100 m in length with excellent resolution (Hawemann et al., 2016). Hand specimens were cut, mechanically polished and scanned with a conventional office-scanner to preserve the context of individual thin sections. Standard thin sections and thin section blocks were SYTON-polished for electron backscatter diffraction (EBSD) analysis. Working conditions for EBSD on uncoated samples were 20 kV, 60 Pa vacuum, ideally 15 mm working distance, and 70° tilt relative to the electron beam on a Quanta 200F scanning electron microscope (SEM) at ScopeM (Scientific center for optical and electron microscopy, ETH Zurich). Chemical indexing (Chi) was performed to improve indexing of feldspar and the data was processed using OIM 7 by EDAX. To remove noise, three types of cleanup techniques were applied: neighbor confidence index correlation, neighbor orientation correlation and grain dilation.

4 Strain localization

4.1 Localization on the lithospheric to kilometer scale

During the Petermann Orogeny, deformation was focused within the interior of the Australian continent, which was already assembled from older cratons by ca. 1300 Ma (Fig. 1; Gray, 1978, Wade et al. 2008). Several mechanisms have been proposed for this first order intracontinental deformation (Raimondo et al., 2014 and references therein). One possibility is thermal weakening caused by heat production from Proterozoic granitic intrusions under a thermal blanket (Hand and Sandiford, 1999). However, the geothermal gradient during the Petermann Orogeny was low (around 17°C, Camacho et al. 1997, Hawemann et al. 2018; Wex et al., 2017) and corresponds to a value typical for stable continental interiors. Sediment thickness on top of the Musgrave Block was also probably not sufficient to create a thermal insulation effect (Camacho et al., 2015). Detrital zircon age populations suggest that the Musgrave Block was at least locally exposed before the Petermann Orogeny (Camacho et al., 2002, 2015) and not fully blanketed by the "Centralian Superbasin", as suggested by Walter et al. (1995). Hand and Sandiford (1999) proposed reactivation of older structures (from the Musgravian Orogeny or Giles Event) as a possible mechanism for localization of deformation in the Musgrave Block. However, in the central Musgrave Block, preserved Musgravian structures are generally steeply dipping and trend N-S, making a link to the E-W trending Petermann shear zones unlikely, and no Giles Event-related structures are currently known from the area. The Petermann Orogeny in the central Musgrave Ranges lacks any magmatism or partial melting, besides quartz-rich pegmatite veins which are limited to the footwall of the Woodroffe Thrust (Wex et al., 2018). Furthermore, the common occurrence of pseudotachylytes argues for a rather strong crust (Camacho et al., 1995). Although the orogen spans a distance of about 200-300 km in a N-S direction between the Officer and Amadeus Basin, exhumation is concentrated in a 20-30 km zone between the Mann Fault and the Woodroffe Thrust, resulting in an extremely narrow, localized core of the Petermann Orogen (Fig. 2a). On the km-scale, it is possible that some dolerite dykes do localize deformation as,

for example, the NDSZ follows a ca. E-W striking series of dykes that is probably part of the Amata dyke suite (our Fig. 3; Camacho, 1997). The DSZ is also bounded to the north by a series of dolerite dykes. Whether the shear zones localized on the dolerite dykes, or the dolerite dykes rotated into the orientation of the shear zones, cannot be answered with confidence. However, most undeformed dykes do not show an E-W orientation, pointing towards reorientation of dykes in the shear zone. On the other hand, the northern boundary of the DSZ has an arcuate shape, which probably requires a pre-existing structure (Fig. 3). The Mann Fault probably localized along the southern boundary of the DSZ, as it follows the same general E-W trend.

4.2 Localization of deformation on lithological heterogeneities

As noted above, some dolerite dykes of the Amata and Alcurra suites possibly localized deformation on the km-scale, whereas many mafic dykes remained undeformed. Although deformation may be focused in these dykes, the boundaries are sometimes also sheared, with the deformation spreading into the adjacent quartzo-feldspathic host rocks (Fig. 4a). This implies some degree of strain hardening during shearing and recrystallization of these metabasic dykes. Older mafic horizons that experienced Musgravian granulite facies metamorphism are coarser grained and did not localize deformation, even when favourably orientated for shearing (Fig. 4b). Instead, narrow fine grained shear zones, generally oriented at a high angle to the shortening direction, cut the boundaries of these layers at a low angle. Quartz-rich pegmatites of unknown age (probably related to the emplacement of Musgravian granitoids), are boudinaged or weakly folded and unsheared (Fig. 4c) in low strain domains. In the mylonite zones, these pegmatites are homogeneously sheared within the country rock, without any discernible tendency for localization. These broader mylonite zones are themselves cross-cut at a low angle in three dimensions by ultramylonite zones, again without preferred localization on quartz-rich veins (Fig. 4d and e). These ultramylonite zones are typically less than a centimeter wide, but can be mapped over lengths of tens of metres.

Figure 4: a) Sheared dolerite dyke with sheared boundaries (26.3408 S, 131.5251 E). b) Undeformed mafic dyke crosscut by narrow shear zones at a high angle to the inferred shortening direction (26.3409 S, 131.5252 E). c) Boudinaged quartz vein or quartz-rich pegmatite in weakly deformed granite (26.3727 S, 131.5531 E). d,e) Mylonitic zone with a set of crosscutting ultramylonite zones and a quartz-rich pegmatite, which is not preferentially sheared (26.3877 S, 131.7073 E)

4.3 Exploitation of pseudotachylytes and fractures during shear zone initiation

Many of the ultramylonites mentioned above preserve features typical of pseudotachylytes, such as injection veins (upper right corner of Fig. 5a) or breccias (Fig. 5b). In Figure 5b, the pseudotachylyte is localized on the boundary between a proto-mylonitic felsic granulite and a dolerite dyke. This pseudotachylyte in turn localized further ductile deformation, as evident from elongated clasts, and was finally brecciated by a younger generation of pseudotachylyte. In otherwise undeformed rocks, planar pseudotachylytes commonly localize all ductile shearing, as seen in Figure 5c, while injection veins evaded shearing. Thicker veins are commonly associated with a damage zone characterized by a high density of small fractures,

along which ductile deformation was also accommodated (Fig. 5d). In area I (Fig. 3), a biotite-rich layer with feldspar augen is observed in a low-strain domain (Fig. 6a). The initial orientation, trending NW-SE, should promote deformation of the layer, if it was weaker, or localize deformation at the boundaries, if it was stronger than the surrounding granite. Instead, the layer shows a thinned intersection zone (compare Pennacchioni and Mancktelow, 2007; their Fig. 10), caused by the interaction of a set of narrow, conjugate shear zones cross-cutting the boundaries of the layer (Fig. 6a,b). The resulting reorientation into an E-W trend is accommodated by a mylonitic foliation both inside the biotite-rich layer and the host rock, with no preferential shearing in either of them. Inside the layer, deformation can be mapped using the feldspar augen as qualitative strain markers, revealing a very heterogeneous distribution of strain along narrow zones of various orientation (Fig. 6b). Outside the high strain zones, two parallel fractures are observed, of which only one shows ductile reactivation (Fig. 6c). Since the resolved shear stress on these parallel features is the same, the most likely interpretation is that fracturing was progressive in time and that the unsheared fractures developed after ductile shearing.

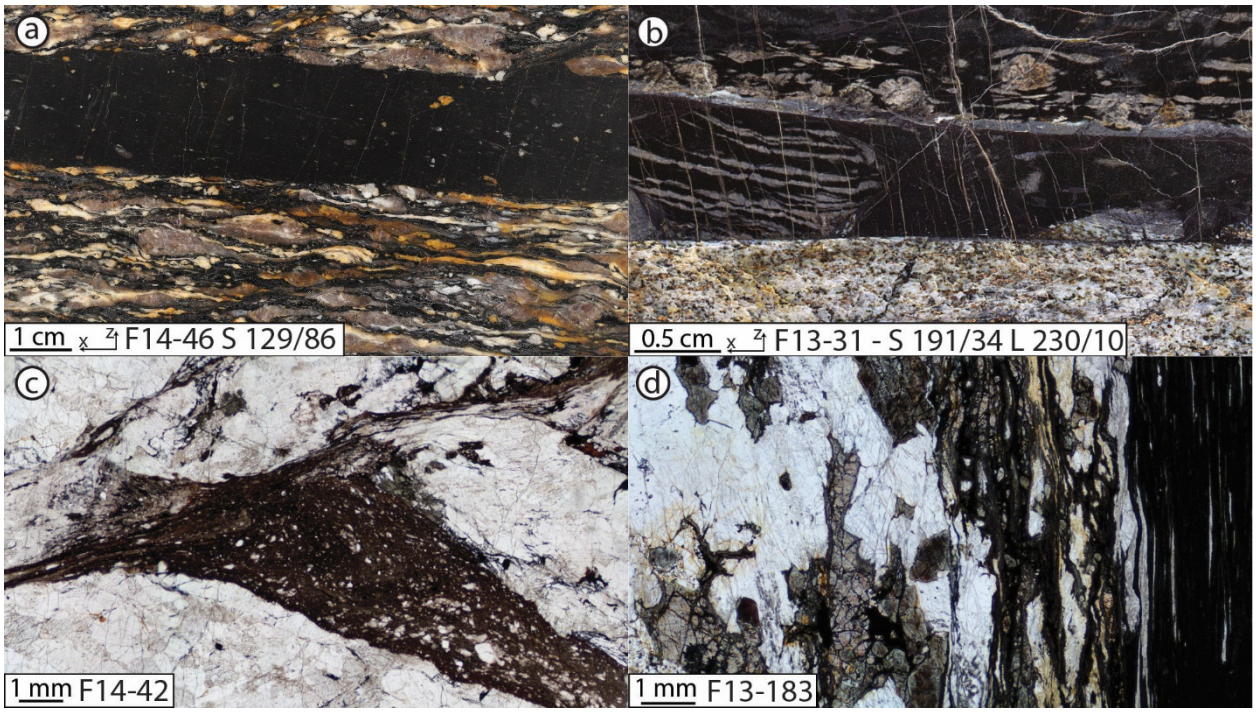

Figure 5: a) Polished hand specimen of a crosscutting pseudotachylyte with a preserved injection vein (upper right) showing minor ductile shearing in a mylonitic granitic host rock (FSZ, 26.4371 S, 131.9707 E). b) Polished hand specimen of a sheared pseudotachylyte at the boundary between a little overprinted felsic granulite and a dolerite dyke, which is brecciated by a second generation of pseudotachylyte (NDSZ, N is up, 26.2793 S, 131.4968 E). c) Sheared pseudotachylyte vein with unsheared injection vein in coarse grained charnockite (FSZ, 26.4454 S, 131.9588 E). d) Strongly sheared pseudotachylyte vein in an otherwise undeformed gabbro (26.3550 S, 131.8398 E). S= schistosity, L= stretching lineation, otherwise not oriented

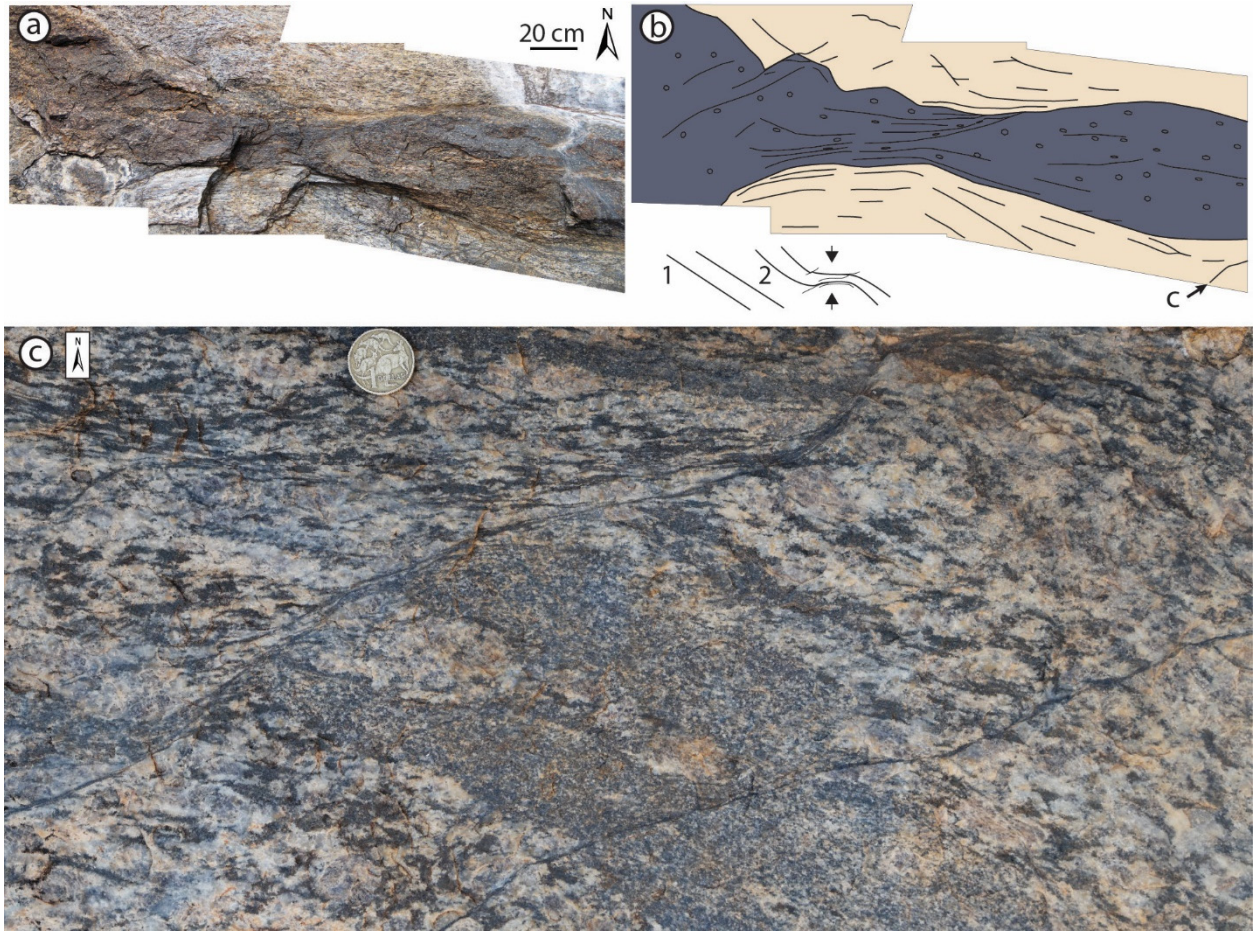

Figure 6: a) Photomosaic of a thinned intersection zone in a biotite-rich layer. b) Sketch of the foliation trend and inferred N-S shortening direction. c) Detail of two parallel fractures, of which only one is ductiley reactivated, from the location indicated in b). Outcrop coordinates: 26.3405 S, 131.5252 E

The relationship between fractures and shear zones can be further illustrated in low strain domains. The outcrop shown in Figure 7a is located in a Musgravian granite that shows almost no background foliation (area II in Fig. 3). The granite hosts aplite dykes, which do not show preferential localization, either inside or at the boundaries. The mapped foliation pattern in Figure 7a is consistent with a dominantly dextral shear zone, with a few minor conjugate sinistral zones. Parallel to these shear zones, fractures are observed, which show reactivation by ductile shear. In most cases, ductile shearing is restricted to the initial length of the fracture (Fig. 7b) but, if the fracture tips are close to each other, they may connect by forming contractional bridges (Fig. 7c; Bürgmann & Pollard, 1994; Pennacchioni, 2005; Segall and Pollard, 1983). This could eventually lead to the formation of a narrow, long shear zone, as observed in the same outcrop. The left-stepping geometry of the initial fractures is consistent with a dextral sense and thus may have been generated in the same stress field as the ductile overprint. Another evidence for the synchronous formation of brittle and ductile deformation is derived from the orientation of Riedel-fractures, indicating the same shortening direction as the ductile overprint (Appendix A1).

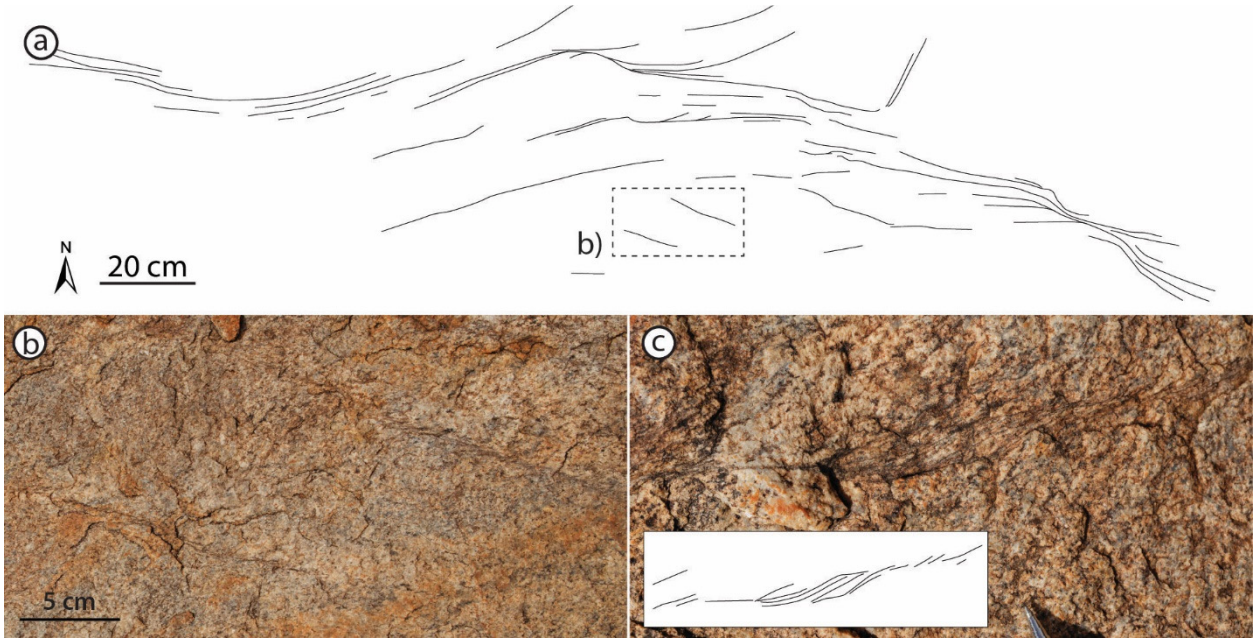

Figure 7: a) Outcrop sketch of the foliation in a narrow shear zone in a little deformed granite. b) Ductilely sheared en-echelon fractures. c) Two fractures connected by a ductile compressional bridge. Outcrop coordinates: 26.3734 S, 131.5622 E

4.4 Late-stage pseudotachylytes localizing on pre-existing structures

Brittle deformation outlasted ductile deformation, with late-stage pseudotachylytes characterized by a black, fine grained but not glassy matrix showing spherulitic to dendritic microstructures typical of quenched melts (Di Toro & Pennacchioni, 2004). This late generation almost exclusively localized on pre-existing planar features, such as lithological boundaries and especially in the rims of dolerite dykes. They can also be emplaced parallel to narrow ultramylonitic shear zones (Fig. 8a), and parallel to foliation planes in broader shear zones (Fig. 8b, see also Glikson & Mernagh, 1990). All these precursor structures generally have a finer grain size than their host rocks.

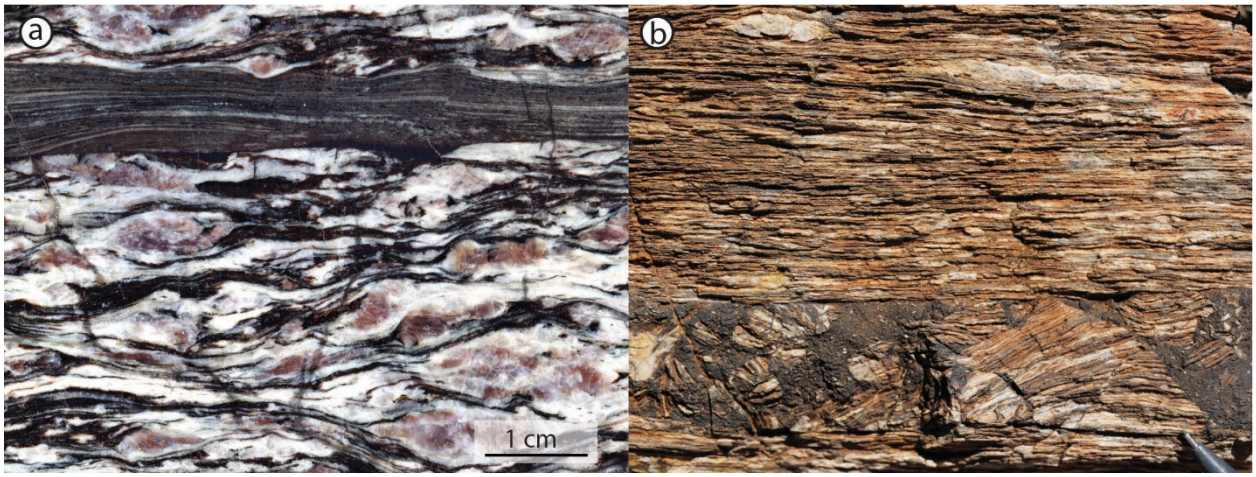

Figure 8: a) Mylonite within a cm-thick ultramylonite band, with pseudotachylyte localized on the lower boundary. Note the microfractures offsetting the ultramylonite (N is up, 26.3882 S, 131.7068 E). b) Pseudotachylyte breccia bounded by the mylonitic foliation (N is up, 26.3640 S, 131.6516 E)

4.5 Summary

With the exception of some fine grained dolerite dykes, shear zones exclusively nucleate, and strain subsequently localized, on fractures and pseudotachylytes. The observation that pseudotachylytes preferentially developed in dolerite dykes, especially along the rims, could imply that pseudotachylyte formation also plays a role in shear localization in the dykes. The angle between the orientations of narrow shear zones and the shortening direction can be very large (Fig. 4b), even where the background strain is low, indicating a large rheological contrast to the relatively undeformed host rock. Dolerite dykes, brittle fractures, and pseudotachylytes are finer grained than the surrounding granitoids and granulites, and all these structures represent long discontinuities with a tabular geometry. These factors seem to be far more important than mineralogical composition, as coarse grained mafic dykes and gabbroic plutons remain unsheared. The amount of water-bearing minerals, such as hornblende and biotite in the granitoids, also does not control strain localization, as these intrusions can locally represent low strain domains. These low-strain domains are readily identified in the field by their smooth and rounded outcrop patterns bounded by strongly foliated high strain zones (Fig. 3). Some fractures appear to be exploited by ductile shearing, while other fractures parallel to these do not show signs of reactivation (e.g. Fig. 6c). Since the resolved shear stress of two planes with the same orientation is the same, all parallel fractures are expected to be sheared if they were rheologically and geometrically similar. The presence of unsheared fractures indicates that fracturing was continuous and coeval with ductile shearing, but in some cases ultimately outlasted ductile deformation.

As discussed in detail in Hawemann et al. (2018), cross cutting sheared pseudotachylytes within shear zones continually developed intermittently during ongoing shearing, in a similar manner to what has been reported elsewhere in other middle (Sibson, 1980; White 1996, 2012) to lower crustal settings (White 2004, 2012). The metamorphic conditions within the sheared pseudotachylyte and the adjacent mylonites are the same (Hawemann et al., 2018), and correspond to upper amphibolite to sub-eclogite facies conditions, typical of lower crustal depths. An important factor is that there is no evidence for hydration during initiation or localization of deformation in these shear zones. In particular, although fractures may be slightly enriched in biotite, there is no development of new muscovite or epidote and no bleached halo along the fracture, which would be typical of fluid-rock interaction, as seen, for example, in “wet” middle crustal examples from the Neves area (Mancktelow and Pennacchioni, 2005; Pennacchioni and Mancktelow, 2007) and Suretta Nappe (Goncalves et al., 2016) in the European Alps. In the Musgrave Ranges, epidote-filled fractures with bleaching halos are common, but postdate the Petermann Orogeny and are most likely related to the Alice Springs Orogeny (~440-340 Ma; Camacho & McDougall, 2000).

5 Non-steady state stress estimates

Texture analysis, using EBSD, provides a detailed analysis of spatially varying grain sizes and subgrain structure, affording a basis for establishing the active deformation, recovery and recrystallization mechanisms and potentially an estimation of the syn-kinematic differential stresses. The sample shown in Figure 9 is a quartzo-feldspathic mylonite with large remnant perthitic K-feldspar clasts (Fig. 9a, upper part). K-feldspar shows fractures decorated with subgrains (Appendix A2). The clasts are mantled by recrystallized grains with outwardly decreasing grain size down to smaller than 1 micron and limited host control on new grain orientation (Appendix A2; compare Viegas et al., 2016). Quartz recrystallized in ribbons of

about 50 micron width by subgrain rotation and subordinate grain boundary migration. For the conditions during shearing of ca. 600-650°C and 1.1-1.2 GPa (Camacho 1997, Hawemann et al., 2018), quartz in water-bearing rocks would be expected to recrystallize predominantly by grain boundary migration (Culshaw & Fyson, 1984; Mancktelow et al., 1998; Schmid & Casey, 1986; Stipp et al., 2002). However, the conditions during localized shearing in the current study area were "dry", without significant fluid-rock interaction or growth of new hydrous minerals. Grain boundary migration is promoted by the presence of a water-rich grain boundary fluid (e.g. Urai et al., 1986) and the transition from dominantly subgrain rotation to dominantly grain boundary migration is thus predicted to occur at higher temperatures under dry conditions (Mancktelow & Pennacchioni, 2004).

The quartz crystallographic preferred orientation (CPO) shown in Figure 9b is strong, with a maximum for the c-axis parallel to Y (the shear zone vorticity axis orthogonal to the stretching lineation and in the shear plane), indicating dominant prism <a> slip (Carter 1976). The effect of subgrain rotation is visible in the rotation of a-axes around c-axes (Fig. 9b) and the development of subgrain boundaries (Fig. 9c,d). While the size of individual grains is on the order of 50-100 micron, the grains show a subgrain structure, with low angle boundaries typically between 5-10° (Fig. 9c,d). These boundaries are also clearly visible on the "image quality" (or pattern contrast) map, since Kikuchi patterns are suppressed along grain boundaries (Fig. 9a, Appendix A3). Large grains internally show an unevenly distributed image quality, indicating high dislocation density (Kunze et al., 1993). The misorientation profile in Figure 9d shows that the change in orientation is discrete across subgrain boundaries and not distributed through the crystal. Calculating a grain size with a threshold of 5° for a (sub-) grain boundary, results in an average grain size of 4.3 microns, but there is a wide spread in observed grain sizes when plotted in terms of area fraction (Fig. 9e). Based on the interpretations of White (1996) and the recent experimental work of Kidder et al. (2016), these observations may reflect a preserved non-steady state grain size, recording a significant change in flow stress between the large grains and the fine subgrains.

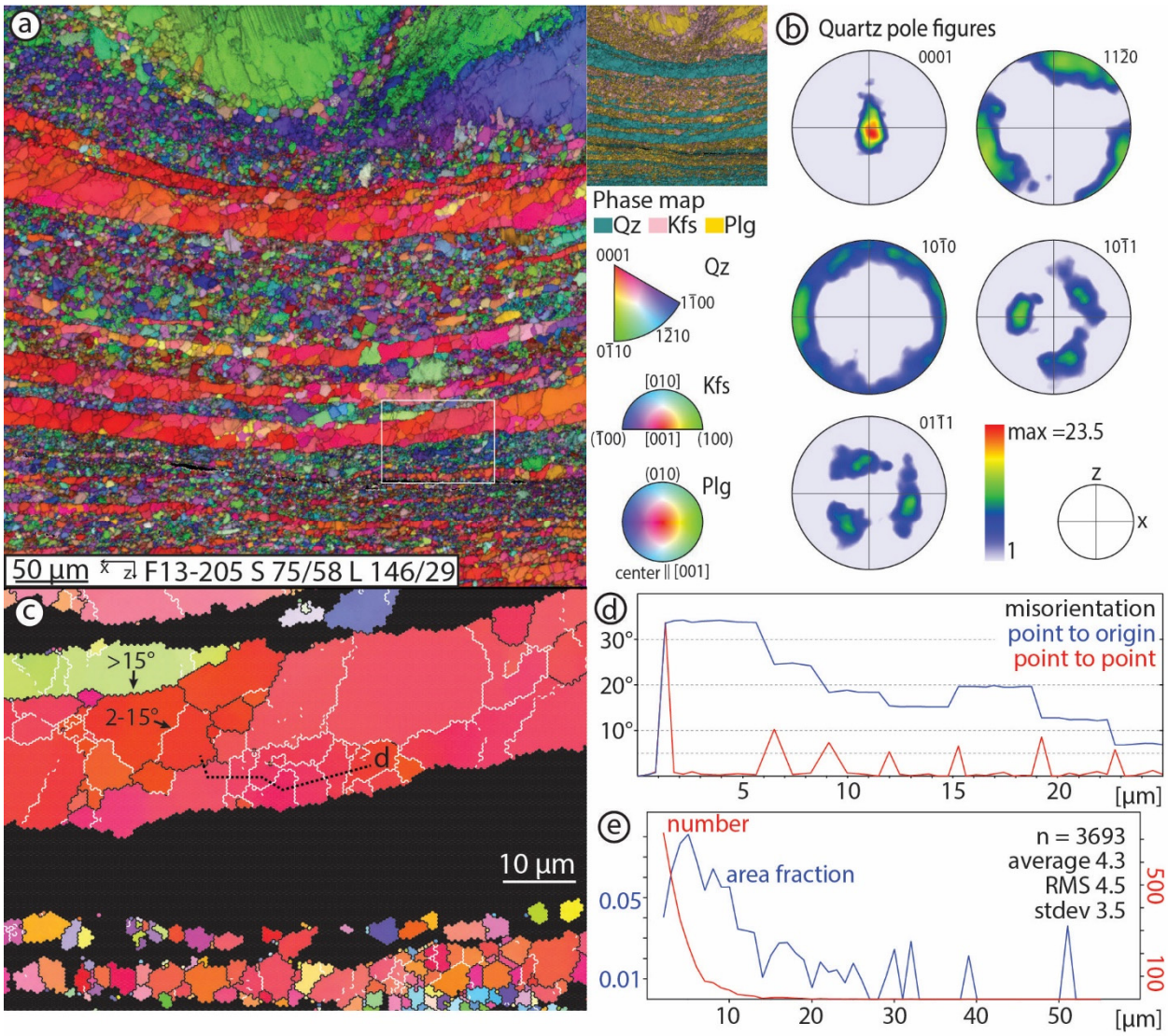

Figure 9: a) Inverse pole figure map with image quality as grey scale and phase map. For inset, see Appendix A2. b) Pole figures for quartz show a Y-maximum. c) Detail of a quartz ribbon (indicated in a) with subgrain boundaries. d) Misorientation profile indicated in c). e) (sub-) grain size chart with grains defined by a 5 degree misorientation.

In many quartz-rich mylonites associated with pseudotachylytes, quartz shows an apparent bimodal grain size distribution (Fig. 10a), in some cases associated with zones showing opposite sense of shear. The coarse grained domains, with grain sizes up to 200 µm, also show subgrains on the order of less than 10 µm, similar to the grain size in the fine-grained domains (Fig. 10b). While this might be interpreted as a later overprint, the CPO of both domains is similar, with a strong Y-maximum for the c-axis (Fig. 10c), pointing to similar conditions during shearing. The grain size distribution chart in Figure 10d reveals a very wide range of grain sizes, between 5 µm and 200 µm.

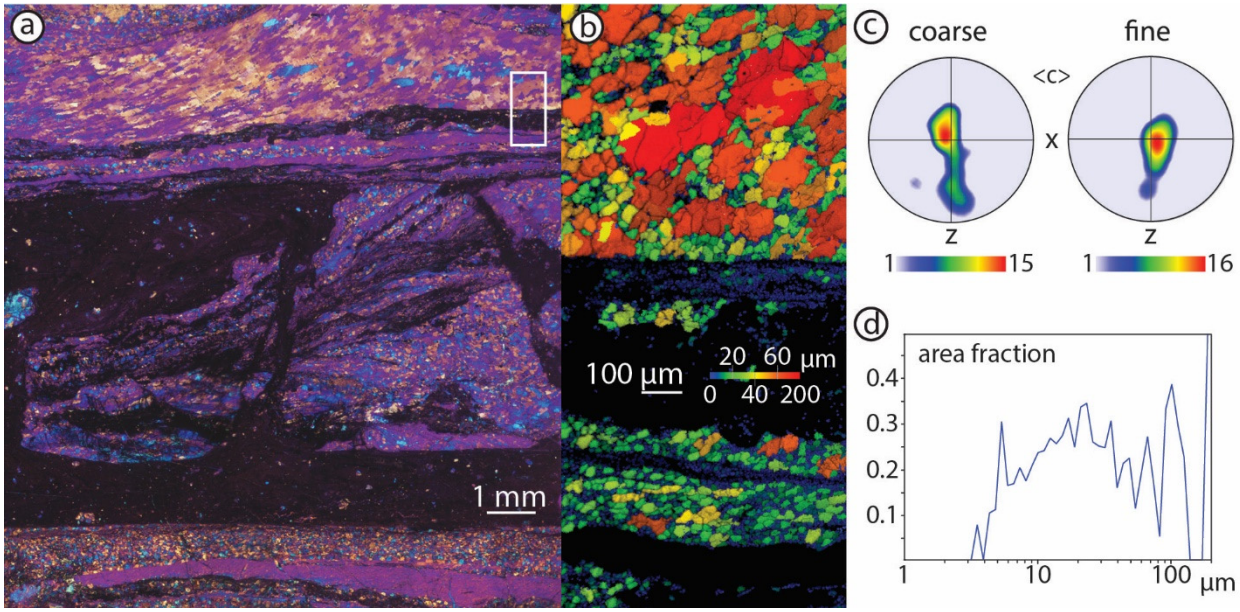

Figure 10: a) Thin section image in crossed polarized light with retardation-plate inserted. While the upper part shows a coarse grain size and dominantly yellow colors, domains with much finer gain sizes exist (blue). Pseudotachylyte is black, with partly rotated clasts. b) Grain size map for quartz, depicting the different domains of large grain size (upper part) with subgrains and small grain size (lower part). The area in between is a garnet-feldspar layer. c) C-axis of quartz for the area b) show a very similar c-axis Y-maximum for quartz. The secondary maximum in the lower part of the coarse grained example probably results from remnant grains, seen as blue spots in the coarse grained ribbon in a). d) Area fraction of grain sizes for quartz shows evenly distributed grain sizes from 5 to 100 micron. In all images, (sub-) grains are defined as domains with > 5° of misorientation between them.

The observation of a cyclic interplay of ductile and brittle deformation poses the question of temporal variations in stress. While the mylonites in the Fregon Subdomain typically show a grain size of 50 to 100 µm, implying stresses on the order of tens of MPa (e.g. Austin and Evans, 2007; Stipp et al., 2006; Stipp and Tullis, 2003; Twiss, 1977), the formation of brittle fractures and pseudotachylytes in dry rock requires stresses on the order of more than 1 GPa (Byerlee, 1978). According to Kidder et al. (2016), quartz grain sizes may record short term stress changes in non-steady state deformation. Stresses calculated from a grain size of 200 µm down to a minimum grain size of 1 µm, are on the order of less than 10 to up to 500 MPa (Austin and Evans, 2007, Stipp and Tullis, 2003).

6 Discussion

An increase in pore fluid pressure can induce fracturing and pseudotachylyte development in the mid- to lower crust (Lund and Austrheim, 2003; Steltenpohl et al., 2006; White, 2012). In the Musgrave Ranges, this fluid driven mechanism cannot explain the formation of pseudotachylytes as the rocks are dry, and there is no evidence for enhanced fluid activity such as coeval veins or hydrous mineral growth. Under dry lower crustal conditions, rocks may be strong (Menegon et al., 2011, Yardley & Valley, 1997;) and this could explain initial fracturing (Menegon et al., 2017), but the stress fluctuations interpreted here cannot be explained by a simple model with persistently strong lower crust. Influx of water-rich fluid along such precursor fractures, causing hydration, associated mineral reactions, and changes in the crystal plastic deformation mechanism(s), has been established as a mean to localize shearing and cause local and bulk weakening of initially dry lower crust (Menegon et al., 2017). However, this is not appropriate in the current study area, where the mineral

assemblage in the shear zones is little changed and there is no evidence for alteration halos or other signs of fluid introduction. The singular and critical change in the precursor fractures is that the grain size is reduced, most dramatically when pseudtotachylyte is also developed.

While the Fregon Subdomain in the study area is mainly dry and shows no signs of water infiltration, the Mulga Park Subdomain (footwall of the Woodroffe Thrust) generally has a higher water content, which increases towards the north (Wex et al., 2018). In addition, Wex et al. (2018) argued that the preferential development of mylonites in the footwall of the thrust can be linked to this higher water content. Counter-intuitively, the thickness of the mylonite zone in the footwall decreases with increasing water content to the north. This could be explained by water weakening mechanisms leading to the localization of the thrust. However, stress estimates are higher in the north than in the south (Wex et al., 2016). Another difference between northern and southern footwall outcrops is the distribution of pseudotachylytes, which appear to more widespread in the south than in the north. Therefore, the thickness of the mylonite zone could be determined by the abundance of pseudotachylyte, with the amount of pseudotachylyte itself controlled by water content. Some authors have proposed that pseudotachylyte preferentially develops in rocks lacking intergranular pore fluid at the time of faulting (Allen, 2005; Barker, 2005; Camacho et al., 1995; Sibson, 1975; Sibson and Toy, 2006). If this is the case, higher water content towards the north could inhibit pseudotachylyte development, thereby leading to the narrower zone of mylonites observed in the north. In this way, the amount of free water influence the thickness of the mylonite zone, but potentially in a more indirect way.

Shear heating is inherent in any permanent deformation and can play a role in strain localization (Braeck and Podladchikov, 2007; Kaus and Podladchikov, 2006). P-T conditions attributed to the Petermann Orogeny from high strain shear zones in the DSZ, moderately deformed and low-strain domains show little variation and overlap within the errors of estimation (Hawemann et al., 2018; Wex et al., 2017). Consequently, there is no retained evidence in the metamorphic minerals for regional-scale shear heating effects.

As noted above, localization on lithological heterogeneities is, with the exception of long, continuous and fine grained dykes, not observed. This implies that the effective viscosity contrast was not large enough to promote localization of deformation on these pre-existing lithological layers. The observations made in the Musgrave Ranges indicate that shear zones initiated on fractures, pseudotachylytes and fine grained dolerite dykes, even when these precursor structures are oriented at a high angle to the shortening direction. Since the resolved shear stress is relatively low, the rheological contrast to the country rock must have been large. What these discontinuities have in common is that they are long, planar in geometry, and have a fine grain size which promotes recrystallization. The observations that (1) ultramylonite zones cross-cut the foliation in coarser grained mylonitic zones in three dimensions at a low angle and (2) that there are multiple cycles of fracturing, pseudotachylyte generation, and crystal-plastic shearing (Hawemann et al., 2018), indicate that stresses were highly variable in time and space. This is further supported by the observation that non-steady state quartz grain sizes vary considerably from a few microns to a few hundred microns. This range can be interpreted to reflect high stresses during pseudotachylyte formation, with nearly instantaneous decay to relatively low stresses during aseismic crystal plastic shearing, followed by a subsequent increase in stress, forming subgrains and micron-sized grains, during later seismic cycles (compare White, 1996).

A common explanation for transient stresses in the mid- to lower crust is the downward propagation of stresses during an earthquake in the seismogenic zone (10-15 km) (e.g. Ellis

and Stöckhert, 2004a,b; White, 1996). However, the large volumes of pseudotachylyte distributed throughout the study area would require a tremendous number of large seismic events in the upper crust (Hawemann et al., 2018). A possible alternative explanation for in-situ generation of high stresses might be stress localization due to jostling of less-deformed strong blocks within the irregular shear zone network (Fig. 11). It is observed on the small scale that fractures with or without pseudotachylytes are a prerequisite for subsequent strain localization. Spreading of deformation by further shear zone nucleation in the intervening blocks may therefore only be possible following fracture at stress concentrations due to interaction between blocks moving on the already developed shear zones. For example, on the large scale, the northern boundary of the Davenport Shear Zone has an arcuate shape, and movement along such a curved and relatively discrete shear zone boundary will cause local stress concentrations between the adjacent blocks. Irregular movement of such blocks can lead to both relative rotation and variation in principal stress directions within blocks, which could explain the difference in preserved shortening direction observed in in the low strain area II in Figure 3. Numerical studies have shown that, due to the interaction of individual shear zone strands, the principal shortening direction inside the shear zones may rotate and lead to further stress perturbations (Meyer et al., 2017).

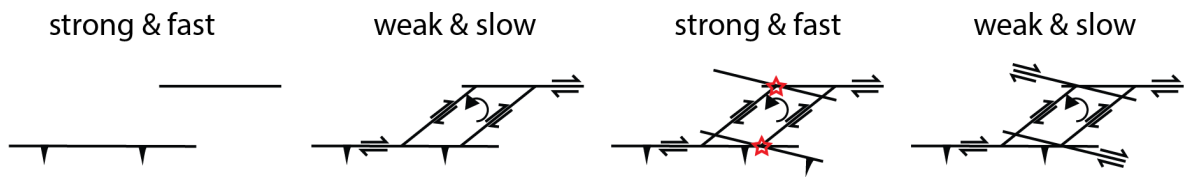

Figure 11: a) Model of the proposed evolution of a shear zone in the study area (scale independent). Pseudotachylytes and fractures are preferred nucleation sites for ductile shearing, resulting in a shear zone network. Block rotation might cause local stress concentration, which are released by fracturing.

The preservation of grains formed at different stresses is generally incomplete, because dynamic and static recrystallisation will tend to erase evidence for previous stages of deformation. Therefore, any study of non-steady state deformation are hampered by the incomplete record of the microstructures. It is, however, remarkable that the small grains in the samples considered in this study survived any later overprint, even though they must have experienced elevated temperature for a significant amount of time. In experimental studies, where rocks are “cooked” after deformation, any evidence for prior deformation is usually erased within a matter of hours to days (Kidder et al., 2016).

Kilian et al. (2017) reported a stress dependence on the crystallographic orientation of quartz grains at constant temperatures. This is in contrast to this study, where the crystallographic orientation is the same in smaller and larger grains (Figs. 9, 10), as was also observed in the earlier study of Fitz Gerald et al. (2006).

7 Conclusions

The distribution of strain observed in the Fregon Subdomain of the Musgrave Block is extremely heterogeneous and localized, with shear zones on a wide range of length scales bounding lower strain intervening blocks. This is in contradiction to common models of crustal rheology, where the lower crust is assumed to deform in a generally weak and

relatively homogeneous manner (Burov and Watts, 2006). In the Fregon Subdomain, strain is highly partitioned and localized along fine grained dolerite dykes, fractures and pseudotachylytes. Rheological heterogeneities, such as coarse grained mafic dykes, aplites or quartz-rich pegmatites did not localize deformation. A recurrent interplay between brittle and ductile deformation and the observation of non-steady state grain sizes imply transient high stress events. Brittle failure of dry rock under lower crustal conditions implies differential stress on the order of GPa. The grain size of quartz in mylonites in the DSZ from the study area is generally relatively coarse (50 to 100 µm) but markedly variable, with grain size ranging from ca. 200 µm down to a measurable minimum grain size of at least 1 µm. This can be interpreted to reflect non-steady-state differential stresses ranging from 10 up to 500 MPa or more. While initial fracturing might be explained by strong behaviour of a dry lower crust, subsequent weakening is indicated by the relatively coarse grain size of quartz in the mylonites. However, low connectivity between the shear zones and relative rotation of low strain domains within this irregular shear zone network might cause stress perturbations along their boundaries. These could explain both the observed interplay between brittle fracturing and ductile flow in the lower crust and the transient elevated stresses implied by pseudotachylytes.

Acknowledgements

We gratefully acknowledge permission granted to work on the Anangu Pitjantjatjara Yankunytjatjara Lands (APY) to carry out our field work in the area. The Northern Territory Geological Survey (NTGS) and Basil Tikoff (Department of Geoscience, University of Wisconsin) are thanked for their logistical support and the Nicolle family of Mulga Park station for their hospitality. The Scientific Center for Optical and Electron Microscopy (ScopeM) provided the facilities for the scanning electron microscopy work, and help by Karsten Kunze is especially acknowledged. Luca Menegon is thanked for his review of the first author's doctoral thesis. This project was financed by the Swiss National Science Foundation (SNF) grant 200021_146745 and by the University of Padova (BIRD175145/17: The geological record of deep earthquakes: the association pseudotachylyte-mylonite).

References

Allen, J. L. (2005). A multi-kilometer pseudotachylyte system as an exhumed record of earthquake rupture geometry at hypocentral depths (Colorado, USA). Tectonophysics, 402(1–4), 37–54. https://doi.org/10.1016/j.tecto.2004.10.017

Austin, N. J., & Evans, B. (2007). Paleowattmeters: A scaling relation for dynamically recrystallized grain size. Geology, 35(4), 343. https://doi.org/10.1130/G23244A.1

Austrheim, H. (1987). Eclogitization of lower crustal granulites by fluid migration through shear zones. Earth and Planetary Science Letters, 81(2–3), 221–232. https://doi.org/10.1016/0012-821X(87)90158-0

Austrheim, Håkon, Erambert, M., & Boundy, T. M. (1996). Garnets recording deep crustal earthquakes. Earth and Planetary Science Letters, 139(1–2), 223–238. https://doi.org/10.1016/0012-821X(95)00232-2

Barker, S. L. L. (2005). Pseudotachylyte-generating faults in Central Otago, New Zealand. Tectonophysics, 397(3), 211–223. https://doi.org/10.1016/j.tecto.2004.12.005

Braeck, S., & Podladchikov, Y. Y. (2007). Spontaneous Thermal Runaway as an Ultimate Failure Mechanism of Materials. Physical Review Letters, 98(9). https://doi.org/10.1103/PhysRevLett.98.095504

Bürgmann, R., & Pollard, D. D. (1994). Strain accommodation about strike-slip fault discontinuities in granitic rock under brittle-to-ductile conditions. Journal of Structural Geology, 16(12), 1655–1674.

Burov, E. B., & Watts, A. B. (2006). The long-term strength of continental lithosphere: “jelly sandwich” or “crème brûlée”? GSA Today, 16(1), 4. https://doi.org/10.1130/1052-5173(2006)016<4:TLTSOC>2.0.CO;2

Byerlee, J. (1978). Friction of rocks. *Pure and Applied Geophysics*, *116*(4–5), 615–626.

Camacho, A. (1997). An Isotopic Study of Deep-Crustal Orogenic Processes: Musgrave Block, Central Australia. PhD Thesis. The Australian National University, Canberra, Australia.

Camacho, A., & Fanning, C. M. (1995). Some isotopic constraints on the evolution of the granulite and upper amphibolite facies terranes in the eastern Musgrave Block, central Australia. Precambrian Research, 71(1), 155–181.

Camacho, A., & McDougall, I. (2000). Intracratonic, strike-slip partitioned transpression and the formation and exhumation of eclogite facies rocks: An example from the Musgrave Block, central Australia. Tectonics, 19(5), 978–996.

Camacho, A., Simons, B., & Schmidt, P. W. (1991). Geological and palaeomagnetic significance of the Kulgera Dyke swarm, Musgrave Block, NT, Australia. Geophysical Journal International, 107(1), 37–45.

Camacho, A., Vernon, R. H., & Fitz Gerald, J. D. (1995). Large volumes of anhydrous pseudotachylyte in the Woodroffe Thrust, eastern Musgrave Ranges, Australia. Journal of Structural Geology, 17(3), 371–383.

Camacho, A., Compston, W., McCulloch, M., & McDougall, I. (1997). Timing and exhumation of eclogite facies shear zones, Musgrave Block, central Australia. Journal of Metamorphic Geology, 15, 735–751.

Camacho, A., Hensen, B. J., & Armstrong, R. (2002). Isotopic test of a thermally driven intraplate orogenic model, Australia. Geology, 30(10), 887. https://doi.org/10.1130/0091-7613(2002)030<0887:ITOATD>2.0.CO;2

Camacho, A., Armstrong, R., Davis, D. W., & Bekker, A. (2015). Early history of the Amadeus Basin: Implications for the existence and geometry of the Centralian Superbasin. Precambrian Research, 259, 232–242. https://doi.org/10.1016/j.precamres.2014.12.004

Carter, N. (1976). Steady State Flow of Rocks. Reviews of Geophysics and Space Physics, 14(3), 301-360.

Christiansen, P. P., & Pollard, D. D. (1997). Nucleation, growth and structural development of mylonitic shear zones in granitic rock. Journal of Structural Geology, 19(9), 1159–1172. https://doi.org/10.1016/S0191-8141(97)00025-4

Collerson, K. D., Oliver, R. L., & Rutland, R. W. R. (1972). An example of structural and metamorphic relationships in the Musgrave orogenic belt, central Australia. Journal of the Geological Society of Australia, 18(4), 379–393. https://doi.org/10.1080/00167617208728776

Culshaw, N. G., & Fyson, W. K. (1984). Quartz ribbons in high grade granite gneiss: modifications of dynamically formed quartz c-axis preferred orientation by oriented grain growth. Journal of Structural Geology, 6(6), 663–668.

Di Toro, G., & Pennacchioni, G. (2004). Superheated friction-induced melts in zoned pseudotachylytes within the Adamello tonalites (Italian Southern Alps). Journal of Structural Geology, 26(10), 1783–1801. https://doi.org/10.1016/j.jsg.2004.03.001

Duretz, T., Schmalholz, S. M., & Podladchikov, Y. Y. (2015). Shear heating-induced strain localization across the scales. Philosophical Magazine, 95(28–30), 3192–3207. https://doi.org/10.1080/14786435.2015.1054327

Edgoose, C. J., Scrimgeour, I. R., Close, D. F., Northern Territory Geological Survey, Northern Territory, & Department of Business, I. & R. D. (2004). Geology of the Musgrave Block, Northern Territory. Darwin, Australia: Northern Territory Geological Survey.

Ellis, S., & Stöckhert, B. (2004a). Elevated stresses and creep rates beneath the brittle-ductile transition caused by seismic faulting in the upper crust. Journal of Geophysical Research, 109(B5). https://doi.org/10.1029/2003JB002744

Ellis, S., & Stöckhert, B. (2004b). Imposed strain localization in the lower crust on seismic timescales. Earth Planets Space, 56(12), 1103–1109.

Evins, P. M., Smithies, R. H., Howard, H. M., Kirkland, C. L., Wingate, M. T. D., & Bodorkos, S. (2010). Redefining the Giles Event within the setting of the 1120-1020 Ma Ngaanyatjarra Rift, West Musgrave Province, Central Australia. East Perth, W.A.: Geological Society of Western Australia.

Fitz Gerald, J. D., Mancktelow, N. S., Pennacchioni, G., & Kunze, K. (2006). Ultrafine-grained quartz mylonites from high-grade shear zones: Evidence for strong dry middle to lower crust. Geology, 34(5), 369. https://doi.org/10.1130/G22099.1

Getsinger, A. J., Hirth, G., Stünitz, H., & Goergen, E. T. (2013). Influence of water on rheology and strain localization in the lower continental crust: Water, Rheology, and Strain Localization. Geochemistry, Geophysics, Geosystems, 14(7), 2247–2264. https://doi.org/10.1002/ggge.20148

Glikson, A. Y., & Mernagh, T. P. (1990). Significance of pseudotachylite vein systems, Giles basic/ultrabasic complex, Tomkinson Ranges, western Musgrave Block, central Australia. Journal of Australian Geology & Geophysics, 11, 509–519.

Goetze, C., & Evans, B. (1979). Stress and temperature in the bending lithosphere as constrained by experimental rock mechanics. Geophysical Journal International, 59(3), 463–478.

Goncalves, P., Oliot, E., Marquer, D., & Connolly, J. a. D. (2012). Role of chemical processes on shear zone formation: an example from the Grimsel metagranodiorite (Aar massif, Central Alps). Journal of Metamorphic Geology, 30(7), 703–722. https://doi.org/10.1111/j.1525-1314.2012.00991.x

Goncalves, Philippe, Poilvet, J.-C., Oliot, E., Trap, P., & Marquer, D. (2016). How does shear zone nucleate? An example from the Suretta nappe (Swiss Eastern Alps). Journal of Structural Geology, 86, 166–180.

Gray, C. M. (1978). Geochronology of granulite-facies gneisses in the western Musgrave Block, Central Australia. Journal of the Geological Society of Australia, 25(7–8), 403–414. https://doi.org/10.1080/00167617808729050

Griggs, D. (1967). Hydrolytic weakening of quartz and other silicates. Geophysical Journal International, 14(1–4), 19–31.

Guermani, A., & Pennacchioni, G. (1998). Brittle precursors of plastic deformation in a granite: an example from the Mont Blanc massif (Helvetic, western Alps). Journal of Structural Geology, 20(2–3), 135–148.

Gueydan, F., Leroy, Y. M., Jolivet, L., & Agard, P. (2003). Analysis of continental midcrustal strain localization induced by microfracturing and reaction-softening. Journal of Geophysical Research: Solid Earth, 108(B2). https://doi.org/10.1029/2001JB000611

Hand, M., & Sandiford, M. (1999). Intraplate deformation in central Australia, the link between subsidence and fault reactivation. Tectonophysics, 305, 121–140.

Hawemann, F., Mancktelow, N., Pennacchioni, G., Wex, S., & Camacho, A. (2016). Bridging scales from satellite to grains: Structural mapping aided by tablet and photogrammetry. In EGU General Assembly Conference Abstracts (Vol. 18, p. 14103).

Hawemann, F., Mancktelow, N. S., Wex, S., Camacho, A., & Pennacchioni, G. (2018). Pseudotachylyte as field evidence for lower-crustal earthquakes during the intracontinental Petermann Orogeny (Musgrave Block, Central Australia). Solid Earth, 9(3), 629–648. https://doi.org/10.5194/se-9-629-2018

Hirth, G., & Tullis, J. (1992). Dislocation creep regimes in quartz aggregates. Journal of Structural Geology, 14(2), 145–159.

Hobbs, B. E., Ord, A., & Teyssier, C. (1986). Earthquakes in the Ductile Regime? PAGEOPH, 124(1), 309–336.

Howard, H. M., Smithies, R. H., Kirkland, C. L., Kelsey, D. E., Aitken, A., Wingate, M. T. D., et al. (2015). The burning heart — The Proterozoic geology and geological evolution of the west Musgrave Region, central Australia. Gondwana Research, 27(1), 64–94. https://doi.org/10.1016/j.gr.2014.09.001

Jackson, J. (2002). Strength of the continental lithosphere: Time to abandon the jelly sandwich? GSA Today, 12(9), 4. https://doi.org/10.1130/1052-5173(2002)012<0004:SOTCLT>2.0.CO;2

Kaus, B. J. P., & Podladchikov, Y. Y. (2006). Initiation of localized shear zones in viscoelastoplastic rocks. Journal of Geophysical Research, 111(B4). https://doi.org/10.1029/2005JB003652

Kidder, S., Hirth, G., Avouac, J.-P., & Behr, W. (2016). The influence of stress history on the grain size and microstructure of experimentally deformed quartzite. Journal of Structural Geology, 83, 194–206. https://doi.org/10.1016/j.jsg.2015.12.004

Kilian, R., & Heilbronner, R. (2017). Analysis of crystallographic preferred orientations of experimentally deformed Black Hills Quartzite. Solid Earth, 8(5), 1095–1117. https://doi.org/10.5194/se-8-1095-2017

Kilian, R., Heilbronner, R., & Stünitz, H. (2011). Quartz grain size reduction in a granitoid rock and the transition from dislocation to diffusion creep. Journal of Structural Geology, 33(8), 1265–1284. https://doi.org/10.1016/j.jsg.2011.05.004

Kirby, S. H. (1983). Rheology of the lithosphere. Reviews of Geophysics, 21(6), 1458. https://doi.org/10.1029/RG021i006p01458

Kronenberg, A. K., Segall, P., & Wolf, G. H. (1990). Hydrolytic weakening and penetrative deformation within a natural shear zone. In A. G. Duba, W. B. Durham, J. W. Handin, & H. F. Wang (Eds.), Geophysical Monograph Series (Vol. 56, pp. 21–36). Washington, D. C.: American Geophysical Union. Retrieved from http://doi.wiley.com/10.1029/GM056p0021

Kunze, K., Wright, S. I., Adams, B. L., & Dingley, D. J. (1993). Advances in automatic EBSP single orientation measurements. Texture, Stress, and Microstructure, 20(1–4), 41–54.

Lund, M. G., & Austrheim, H. (2003). High-pressure metamorphism and deep-crustal seismicity: evidence from contemporaneous formation of pseudotachylytes and eclogite facies coronas. Tectonophysics, 372(1–2), 59–83. https://doi.org/10.1016/S0040-1951(03)00232-4

Maboko, M. A. H., McDougall, I., Zeitler, P. K., & Williams, I. S. (1992). Geochronological evidence for ~ 530–550 Ma juxtaposition of two Proterozoic metamorphic terranes in the Musgrave Ranges, Central Australia. Australian Journal of Earth Sciences, 39(4), 457–471. https://doi.org/10.1080/08120099208728038

Major, R. B., & Conor, C. H. H. (1993). The Precambrian. In J. F. Drexel, W. V. Preiss, & A. J. Parker (Eds.), The geology of South Australia (Vol. 1, pp. 156–167). Geological Survey of South Australia.

Mancktelow, N. S., & Pennacchioni, G. (2004). The influence of grain boundary fluids on the microstructure of quartz-feldspar mylonites. Journal of Structural Geology, 26(1), 47–69. https://doi.org/10.1016/S0191-8141(03)00081-6

Mancktelow, N. S., & Pennacchioni, G. (2005). The control of precursor brittle fracture and fluid–rock interaction on the development of single and paired ductile shear zones. Journal of Structural Geology, 27(4), 645–661. https://doi.org/10.1016/j.jsg.2004.12.001

Mancktelow, N. S., & Pennacchioni, G. (2013). Late magmatic healed fractures in granitoids and their influence on subsequent solid-state deformation. Journal of Structural Geology, 57, 81–96. https://doi.org/10.1016/j.jsg.2013.09.006

Mancktelow, N. S., Grujic, D., & Johnson, E. L. (1998). An SEM study of porosity and grain boundary microstructure in quartz mylonites, Simplon Fault Zone, Central Alps. Contributions to Mineralogy and Petrology, 131(1), 71–85.

Menegon, L., Pennacchioni, G., Malaspina, N., Harris, K., & Wood, E. (2017). Earthquakes as Precursors of Ductile Shear Zones in the Dry and Strong Lower Crust. Geochemistry, Geophysics, Geosystems, 18(12), 4356–4374. https://doi.org/10.1002/2017GC007189

Menegon, Luca, Nasipuri, P., Stünitz, H., Behrens, H., & Ravna, E. (2011). Dry and strong quartz during deformation of the lower crust in the presence of melt. Journal of Geophysical Research, 116(B10). https://doi.org/10.1029/2011JB008371

Menegon, Luca, Pennacchioni, G., Harris, K., & Wood, E. (2014). High temperature pseudotachylytes and ductile shear zones in dry rocks from the continental lower crust (Lofoten, Norway). In EGU General Assembly Conference Abstracts (Vol. 16, p. 12810). Retrieved from http://adsabs.harvard.edu/abs/2014EGUGA..1612810M

Meyer, S. E., Kaus, B., & Passchier, C. (2017). Development of branching brittle and ductile shear zones: A numerical study. Geochemistry, Geophysics, Geosystems. https://doi.org/10.1002/2016GC006793

Nakamura, A., & Milligan, P. R. (2016). Total Magnetic Intensity (TMI) image 2015 greyscale. Commonwealth of Australia (Geoscience Australia). https://doi.org/10.4225/25/574CF5E15C119

Nazareth, J. J., & Hauksson, E. (2004). The seismogenic thickness of the southern California crust. Bulletin of the Seismological Society of America, 94(3), 940–960.

Pennacchioni, G., Di Toro, G., Brack, P., Menegon, L., & Villa, I. M. (2006). Brittle–ductile–brittle deformation during cooling of tonalite (Adamello, Southern Italian Alps). Tectonophysics, 427(1–4), 171–197. https://doi.org/10.1016/j.tecto.2006.05.019

Pennacchioni, Giorgio. (2005). Control of the geometry of precursor brittle structures on the type of ductile shear zone in the Adamello tonalites, Southern Alps (Italy). Journal of Structural Geology, 27(4), 627–644. https://doi.org/10.1016/j.jsg.2004.11.008

Pennacchioni, Giorgio, & Mancktelow, N. S. (2007). Nucleation and initial growth of a shear zone network within compositionally and structurally heterogeneous granitoids under amphibolite facies conditions. Journal of Structural Geology, 29(11), 1757–1780. https://doi.org/10.1016/j.jsg.2007.06.002

Pennacchioni, Giorgio, & Zucchi, E. (2013). High temperature fracturing and ductile deformation during cooling of a pluton: The Lake Edison granodiorite (Sierra Nevada batholith, California). Journal of Structural Geology, 50, 54–81. https://doi.org/10.1016/j.jsg.2012.06.001

de Raadt, W. S., Burlini, L., Kunze, K., & Spiers, C. J. (2014). Effect of pre-existing crystallographic preferred orientation on the rheology of Carrara marble. Journal of Structural Geology, 68, 44–57. https://doi.org/10.1016/j.jsg.2014.07.011

Raimondo, T., Hand, M., & Collins, W. J. (2014). Compressional intracontinental orogens: Ancient and modern perspectives. Earth-Science Reviews, 130, 128–153. https://doi.org/10.1016/j.earscirev.2013.11.009

Ranalli, G., & Murphy, D. C. (1987). Rheological stratification of the lithosphere. Tectonophysics, 132(4), 281–295.

Schmid, S. M., & Casey, M. (1986). Complete fabric analysis of some commonly observed quartz c-axis patterns. Geophysical Monograph Series, 36, 263–286.

Schmidt, P. W., Williams, G. E., Camacho, A., & Lee, J. K. W. (2006). Assembly of Proterozoic Australia: implications of a revised pole for the ~1070 Ma Alcurra Dyke Swarm, central Australia. Geophysical Journal International, 167(2), 626–634. https://doi.org/10.1111/j.1365-246X.2006.03192.x

Schrank, C. E., Handy, M. R., & Fusseis, F. (2008). Multiscaling of shear zones and the evolution of the brittle-to-viscous transition in continental crust. Journal of Geophysical Research: Solid Earth, 113(B1), B01407. https://doi.org/10.1029/2006JB004833

Segall, P., & Pollard, D. D. (1983). Nucleation and growth of strike slip faults in granite. Journal of Geophysical Research, 88(B1), 555. https://doi.org/10.1029/JB088iB01p00555

Sibson, R. H. (1980). Transient discontinuities in ductile shear zones. Journal of Structural Geology, 2(1), 165–171.

Sibson, Richard H. (1975). Generation of pseudotachylyte by ancient seismic faulting. Geophysical Journal International, 43(3), 775–794.

Sibson, Richard H. (1982). Fault zone models, heat flow, and the depth distribution of earthquakes in the continental crust of the United States. Bulletin of the Seismological Society of America, 72(1), 151–163.

Sibson, Richard H., & Toy, V. G. (2006). The habitat of fault-generated pseudotachylyte: Presence vs. absence of friction-melt. In R. Abercrombie, A. McGarr, H. Kanamori, & G. Di Toro (Eds.), Geophysical Monograph Series (Vol. 170, pp. 153–166). Washington, D. C.: American Geophysical Union. Retrieved from http://www.agu.org/books/gm/v170/170GM16/170GM16.shtml

Smithies, R. H., Howard, H. M., Evins, P. M., Kirkland, C. L., Kelsey, D. E., Hand, M., et al. (2011). High-Temperature Granite Magmatism, Crust-Mantle Interaction and the Mesoproterozoic Intracontinental Evolution of the Musgrave Province, Central Australia. Journal of Petrology, 52(5), 931–958. https://doi.org/10.1093/petrology/egr010

Steltenpohl, M. G., Kassos, G., & Andresen, A. (2006). Retrograded eclogite-facies pseudotachylytes as deep-crustal paleoseismic faults within continental basement of Lofoten, north Norway. Geosphere, 2(1), 61–72. https://doi.org/10.1130/GES00035.1

Stewart, M., Holdsworth, R. E., & Strachan, R. A. (2000). Deformation processes and weakening mechanisms within the frictional–viscous transition zone of major crustal-scale faults: insights from the Great Glen Fault Zone, Scotland. Journal of Structural Geology, 22(5), 543–560.

Stipp, M., & Tullis, J. (2003). The recrystallized grain size piezometer for quartz. Geophysical Research Letters, 30(21). https://doi.org/10.1029/2003GL018444

Stipp, M., Stünitz, H., Heilbronner, R., & Schmid, S. M. (2002). The eastern Tonale fault zone: a 'natural laboratory' for crystal plastic deformation of quartz over a temperature range from 250 to 700°C. Journal of Structural Geology, 24(12), 1861–1884. https://doi.org/10.1016/S0191-8141(02)00035-4

Stipp, M., Tullis, J., & Behrens, H. (2006). Effect of water on the dislocation creep microstructure and flow stress of quartz and implications for the recrystallized grain size piezometer. Journal of Geophysical Research, 111(B4). https://doi.org/10.1029/2005JB003852

Thielmann, M., Rozel, A., Kaus, B. J. P., & Ricard, Y. (2015). Intermediate-depth earthquake generation and shear zone formation caused by grain size reduction and shear heating. Geology, 43(9), 791–794. https://doi.org/10.1130/G36864.1

Twiss, R. J. (1977). Theory and applicability of a recrystallized grain size paleopiezometer. Pure and Applied Geophysics PAGEOPH, 115(1–2), 227–244. https://doi.org/10.1007/BF01637105

Urai, J. L., Means, W. D., & Lister, G. S. (1986). Dynamic recrystallization of minerals. In B. E. Hobbs & H. C. Heard (Eds.), Geophysical Monograph Series (Vol. 36, pp. 161–199). Washington, D. C.: American Geophysical Union.

Viegas, G., Menegon, L., & Archanjo, C. (2016). Brittle grain-size reduction of feldspar, phase mixing and strain localization in granitoids at mid-crustal conditions (Pernambuco shear zone, NE Brazil). Solid Earth, 7(2), 375–396. https://doi.org/10.5194/se-7-375-2016

Wade, B. P., Kelsey, D. E., Hand, M., & Barovich, K. M. (2008). The Musgrave Province: Stitching north, west and south Australia. Precambrian Research, 166(1–4), 370–386. https://doi.org/10.1016/j.precamres.2007.05.007

Walter, M. R., Veevers, J. J., Calver, C. R., & Grey, K. (1995). Neoproterozoic stratigraphy of the centralian superbasin, Australia. Precambrian Research, 73(1–4), 173–195.

Wex, S., Mancktelow, N. S., Hawemann, F., Camacho, A., & Pennacchioni, G. (2016). Interplay between Seismic Fracturing and Aseismic Creep in the Woodroffe Thrust, Central Australia – Inferences for the Rheology of Relatively "Dry" Middle Continental Crust. AGU Fallmeeting 2016, T21E-03. San Francisco, USA.

Wex, S., Mancktelow, N. S., Hawemann, F., Camacho, A., & Pennacchioni, G. (2017). Geometry of a large-scale, low-angle, mid-crustal thrust (Woodroffe Thrust, central Australia): Geometry of a mid-crustal thrust. Tectonics. https://doi.org/10.1002/2017TC004681

White, J. C. (2004). Instability and localization of deformation in lower crust granulites, Minas fault zone, Nova Scotia, Canada. Geological Society, London, Special Publications, 224(1), 25–37. https://doi.org/10.1144/GSL.SP.2004.224.01.03

White, Joseph Clancy. (1996). Transient discontinuities revisited: pseudotachylyte, plastic instability and the influence of low pore fluid pressure on deformation processes in the mid-crust. Journal of Structural Geology, 18(12), 1471–1486.

White, Joseph Clancy. (2012). Paradoxical pseudotachylyte – Fault melt outside the seismogenic zone. Journal of Structural Geology, 38, 11–20. https://doi.org/10.1016/j.jsg.2011.11.016

Wingate, M. T., Campbell, I. H., Compston, W., & Gibson, G. M. (1998). Ion microprobe U–Pb ages for Neoproterozoic basaltic magmatism in south-central Australia and implications for the breakup of Rodinia. Precambrian Research, 87(3), 135–159.

Yardley, B. W. D., & Valley, J. W. (1994). How wet is the Earth's crust? Nature, 371(6494), 205–206. https://doi.org/10.1038/371205a0

Yardley, B. W. D., & Valley, J. W. (1997). The petrologic case for a dry lower crust. Journal of Geophysical Research: Solid Earth, 102(B6), 12173–12185. https://doi.org/10.1029/97JB00508

Zhao, J., & McCulloch, M. (1993). Sm-Nd mineral isochron ages of Late Proterozoic dyke swarms in Australia: evidence for two distinctive events of mafic magmatism and crustal extension. Chemical Geology, 109, 341–354.

Zhao, J., McCulloch, M., & Korsch, R. J. (1994). Characterisation of a plume-related ~ 800 Ma magmatic event and its implications for basin formation in central-southern Australia. Earth and Planetary Science Letters, 121, 349–367.

Appendix A

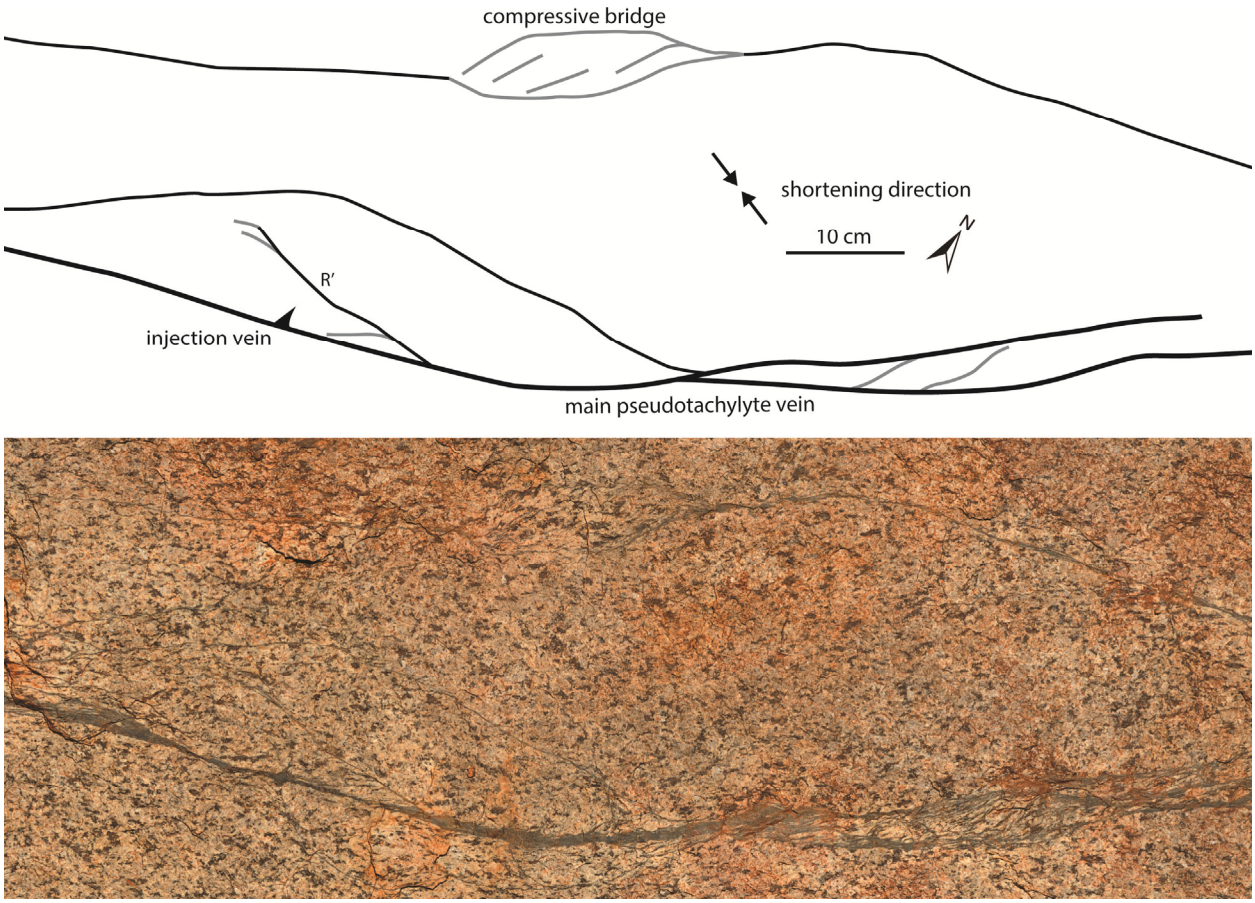

Appendix A1: Outcrop in a low strained granite with a sheared pseudotachylyte vein (25.9980 S, 131.7463 E). The shortening direction for both, brittle and ductile deformation are the same, as seen from riedel-type fractures and the orientation of the compressive bridge.

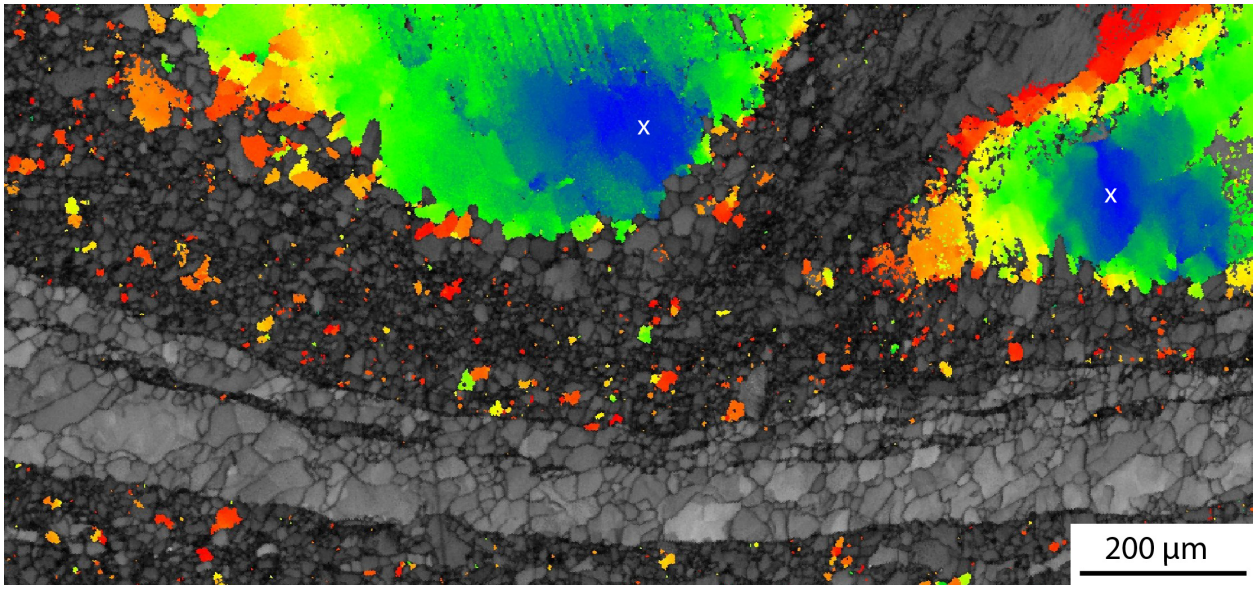

Appendix A2: Misorientation map with respect to the reference points (x), for the feldspar clast in Fig. 9a, reveals that mantle grains do not inherit the orientation from the host grain. Misorientation angle from blue=0° to red=10°.

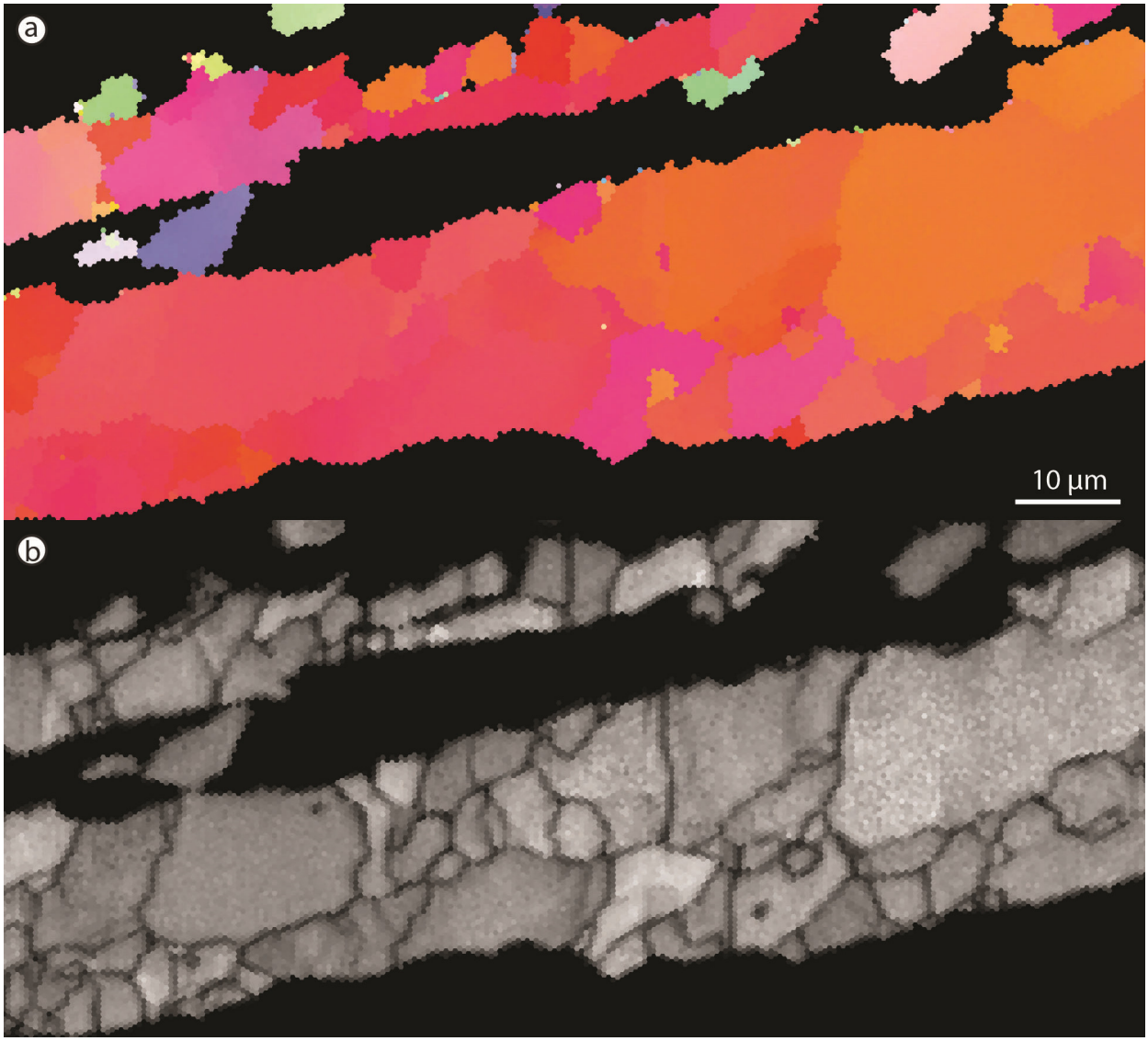

Appendix A3: Inset of Figure 9a. a) Inverse pole figure map, for colours see Figure 9a. b) "Image quality"-map reveals subgrain boundaries which remain invisible in a).